Endocrine Journal 2017, **64** (5), 543-552

ORIGINAL

The effects of metformin on fibroblast growth factor 19, 21 and fibroblast growth factor receptor 1 in high-fat diet and streptozotocin induced diabetic rats

Yan Wang[1), 2)], Ningning Dang[3)], Pei Sun[2)], Jin Xia[2), 4)], Chunxue Zhang[2), 4)] and Shuguang Pang[1), 2), 4)]

[1)] *School of Medicine, Shandong University, Jinan 250013, Shandong Province, China*
[2)] *Department of Endocrinology, Jinan Central Hospital Affiliated to Shandong University, Jinan 250013, Shandong Province, China*
[3)] *Department of Dermatology, Jinan Central Hospital Affiliated to Shandong University, Jinan 250013, Shandong Province, China*
[4)] *Department of Medicine, Taishan Medical University, Taian 271000, Shandong Province, China*

Abstract. To understand metformin's effects on fibroblast growth factors (FGFs) and fibroblast growth factor receptor 1 (FGFR1), we investigated circulating fibroblast growth factor-19 (FGF19), FGF21 levels, and FGFR1 in type 2 diabetes mellitus (T2DM). In addition, protein kinase B (Akt) signaling pathway was detected to explain the possible mechanisms. T2DM was induced by feeding rats with high-fat diet for 11 weeks, followed by a low dose of streptozotocin (STZ, 30-35 mg/kg, intraperitoneally). Control rats (Con) were fed on a normal chow; diabetic rats (DM) were fed on high-fat diet supplemented with or without metformin (METF) for 12 weeks (500 $mg \cdot kg^{-1} \cdot d^{-1}$). Biochemical parameters were detected at the end of 24th weeks. FGFR1 expression and protein kinase B (Akt) phosphorylation in the pancreas and visceral adipose tissues were detected using either Western blot (WB) or immunohistochemistry (IHC). Serum FGF19 and FGF21 were measured using enzyme-linked immune sorbent assay (ELISA). Metformin treated DM rats showed improved glucose, lipid and bile acid metabolism. Besides, significantly decreased FGF19 and increased FGF21 were observed in DM+METF rats. DM rats showed significantly increased FGFR1 both in the pancreas and visceral adipose tissues. While in DM+METF rats, FGFR1 was almost remained at a normal level in the pancreas and increased in the visceral adipose tissue compared to that in DM rats. Besides, metformin treatment restores Akt phosphorylation in both tissues. The altered glucose and lipid profiles by metformin treatment may be associated with the increased circulating FGF21 and tissue-specific expressions of FGFR1.

Key words: Diabetes, FGF21, FGFR1, β cell, Visceral adipose

TYPE 2 DIABETES MELLITUS (T2DM) is associated with obesity and insulin resistance and has severe complications. As an effective and safe oral drug, metformin has been used to treat T2DM for almost fifty years. Possible mechanisms of metformin in improving glucose homeostasis are partially depended on the activation of adenosine monophosphate-activated protein kinase (AMPK) which then inhibits glucose output and increases insulin sensitivity in peripheral tissues [1].

Fibroblast growth factor-19 (FGF19) and FGF21 belong to beta-klotho family, and recent studies showed that they were produced by the activation of Farnesoid X Receptor (FXR) in the ileum and liver, respectively [2, 3]. FGF19 and FGF21 are emerging as endocrine hormones since they showed novel roles in bile acid, lipid, and glucose metabolism [4-6]. In obese or diabetic animal models, administration of FGF19 and FGF21 led to beneficial effects on metabolism through increasing insulin sensitivity, energy expenditure and white adipose browning [7-10].

FGFs exert their roles by binding to different receptors. Fibroblast growth factor receptors (FGFRs) consist of FGFR1, FGFR2, FGFR3 and FGFR4. By binding to FGFR4, FGF19 inhibits CYP7A1, the rate limiting enzyme of bile acid biosynthesis, thus inhibiting bile acid synthesis. In addition, previous study showed that selective activation of FGFR4 failed to improve glucose metabolism in *ob/ob* mice [11]. Thus,

Submitted Aug. 16, 2016; Accepted Feb. 3, 2017 as EJ16-0391
Released online in J-STAGE as advance publication Apr. 11, 2017
Correspondence to: Shuguang Pang, M.D., Ph.D., Department of Endocrinology, Jinan Central Hospital Affiliated to Shandong University, 105 Jiefang Road, Jinan 250013, Shandong Province, China. E-mail: shuguangpang@163.com

emerged roles of FGFR1 in lipid and glucose metabolism have come into notice [12, 13].

FGFR1 is mainly expressed in the pancreas and adipose tissues. Hart *et al*. suggested that in the pancreas, FGFR1 is predominantly located in the β cell and attenuation of FGFR1 signaling leads to β cell dysfunction, thus leading to diabetes [14]. Besides, ablation of FGFR1 in adipose tissue resulted in impaired lipid profile [15]. Moreover, FGFR1 agonist treated diabetic mice exhibited improvement of hyperglycemia, hyperlipidemia, and hepatosteatosis [16]. Therefore, rescuing FGFR1 signaling would provide opportunity to reverse T2DM.

Material and Methods

Materials

Metformin was purchased from Bristol-Myers Squibb. Streptozotocin (STZ) was purchased from Sigma (USA). Antibodies against FGFR1 (9740s), Akt (#9272) and phospho-Akt (p-Akt) (Ser 473, #4060) were purchased from Cell Signaling Technology Inc. (Danvers, MA, USA); antibody against β-actin was from ZSJQ-Bio (Beijing, China). Rat FGF19 and FGF21 ELISA kits were purchased from Jianglai-Bio (Shanghai, China).

Animal experiments

Male Wistar rats (8 w, 220-250 g) were purchased from Vital River Laboratory Animal Technology Co. Ltd. (Beijing, China). The rats were maintained at room temperature (25°C) and in 12-hour light and 12-hour dark cycle with free access to water and chow. After one week of dietary accommodation, the experimental rats were randomly assigned to three groups of twenty animals each: control rats group (Con), diabetic rats group (DM) and metformin treated diabetic rats group (DM+METF). Con rats were fed with normal diet, while DM and DM+METF rats with high-fat diet. After HFD administration for 11 weeks, DM and DM+METF rats received a low dose of STZ intraperitoneal injection (30-35 mg/kg, Sigma) to induce diabetes model. After STZ injection, the animals were deprived of food for 12 h. Diabetes was regarded as successfully induced in rats with fasted blood glucose levels > 11.1 mmol/L. DM+METF rats were given metformin (500 $mg \cdot kg^{-1} \cdot d^{-1}$) by oral gavage for 12 weeks after diabetes model induction. The normal diet consists of 6% fat, 64% carbohydrate and 23% protein, whereas high fat diet consists of 25% fat, 48% carbohydrate and 20% protein. At 32 weeks of age, all rats were fasted overnight before serum and tissue collection. Serum and tissues were removed and frozen in -80°C or liquid nitrogen. Body mass and food intake were determined every other day. All animal protocols in the experiment were conducted with the approval of Animal Study Committee of Shandong University.

Biochemical analysis

Insulin enzyme-linked immunosorbent assay (ELISA) test kits (Art, No.10-1250-01) were purchased from Mercodia (Uppsala, Sweden), and the serum insulin (FIN) detection was carried out following the manufactures' instruction. At the age of 32 weeks, rats were fasted for 16 hours. Fasting blood glucose (FBG), total cholesterol (TC), triglyceride (TG), high-density lipoprotein cholesterol (HDL-C), low-density lipoprotein cholesterol (LDL-C), and total bile acids (TBAs) were detected using cobas8000 automatic biochemistry analyzer (Roche, Basel, Switzerland). Blood glucose level was detected using glucose testing strips and analyzed by the tool of glucometer (Roche, Basel, Switzerland).

Oral glucose tolerance test

After 24 weeks of interference, rats were anesthetized with ether. For OGTT, rats were given 2 g/kg glucose by oral gavage. Then blood samples were collected 0, 30, 60, 120 minutes after oral glucose through retroorbital plexus for the measurement of glucose and insulin. The homeostatic model assessment of insulin resistance (HOMA-IR) index was calculated as [FBG (mmol/L) × FIN (μU/mL)] / 22.5 to assess insulin resistance.

Enzyme linked immunosorbent assay

At the end of the experiment, all rats were fasted overnight before serum collection. After anesthetized with ether, blood samples by eye angular vein were harvested and transferred on ice immediately and centrifuged for 10 min at 3,000 g/min at 4°C. The supernatant was collected and stored at -80°C. The preserved serum samples were added to a 48-well plate to examine FGF19 and FGF21 by using ELISA kits (Jianglai-Bio, Shanghai, China) according to the manufacture's manual. Briefly, all ELISA reagents and frozen samples were brought to the room temperature, then samples were diluted 1:5 with diluent solution.

50 μL of supernatant diluent, positive and negative control were added into each well and incubated at 37°C for 30 minutes. The procedure continued by manually washing the wells five times with washing buffer reagent. Then an amount of 50 μL of enzyme conjugate reagent was immediately added to the wells and incubated at 37°C for 30 minutes. The plates were washed five times with washing buffer reagent. After the last wash, chromogen reagent was added to each well and incubated in the dark room for 15 minutes at 37°C. The reaction was stopped by adding 50 μL stop buffer and recorded at 450 nm using microplate reader (Biorad, USA). Each standard and experimental sample was run in duplicate and the results were averaged.

Western blot analysis

The extraction and isolation of islet and visceral adipose proteins were lysed with RIPA (Beyotime, Beijing, China) supplemented with 1 mM PMSF (Solarbio, Beijing, China) on ice and centrifuged for 10 min at 14,000 g/min at 4°C. The precipitate was removed by centrifugation, and the supernatant was collected for Western blot.

Total protein concentration was quantified and equal amounts of protein were loaded on 8%-10% SDS-PAGE and transferred onto PVDF membranes (0.2mm, Millipore, Billerica, MA, USA). After membranes were blocked, they were incubated for 24 h at 4°C with the primary antibodies against FGFR1, Akt, p-Akt followed by HRP conjugated secondary antibody for 1.5 h at room temperature. Protein bands were detected using an ECL detection kit (Millipore, Billerica, MA, USA). Normalization of total protein expression was carried out by using β-actin as control. Data are shown representative of 3-5 independent experiments. Blot results were presented as direct band comparisons in autoradiographs and quantified by densitometry using the Image J software (NIH, Bethesda, MD, USA).

Immunohistochemistry

Images of pancreatic sections immunostained by anti-FGFR1 antibody were subjected to analyze FGFR1 expression. Fresh islet samples were immediately fixed in neutral formalin and embedded in paraffin. Paraffin-embedded samples were cut into 5-μm sections. After that, slides were deparaffinized and rehydrated in serial dilutions of ethanol, placed in antigen retrieval solution and microwaved at low power for 10 min. Then, slides were incubated in 3% H_2O_2 for 10 minutes to block endogenous peroxidase. After that, slides were washed for 5 minutes in phosphate-buffered saline (PBS) and blocked for 30 minutes at room temperature with 3% blocking serum in PBS. A rat monoclonal antibody against FGFR1 was added and incubated at 4°C overnight. Sections were then incubated with a horseradish peroxidase (HRP)-conjugated goat anti-rat antibody for 30 min at 37°C. The antibody binding was visualized by 3, 3-diaminobenzidine (Dako, Denmark) as a chromogenic substrate. The slides were then counterstained with hematoxylin. As a negative control, duplicate sections were stained without exposure to the primary antibodies. Images of the sections were captured using a microscope. A brown or yellow color was regarded as a positive reaction. Immunohistochemical analysis was performed using Image-Pro Plus 6.0 (Media Cybernetics, Silver Spring, USA). The percentage of stained areas were recorded by counting at least five screens of each slice under a magnification of 200×. And the average integrated optical density (IOD) values in each group were collected and analyzed. The results were analyzed with GraphPad Prsism 6.0 software (Graphpad Software, Inc., San Diego, CA, USA).

Data analysis

All numerical results were expressed as means ± SEM. Blot results were presented as direct band comparisons in autoradiographs and quantified by densitometry using the Image J software (NIH, Bethesda, MD, USA). Comparisons among three groups were achieved *via* one-way analysis of variance (ANOVA) followed by Dunnett's test. $p<0.05$ was considered statistically significant. All statistical analyses were performed with GraphPad Prsism 6.0 software (Graphpad Software, Inc., San Diego, CA, USA).

Results

Effects of metformin on food intake and body weight

Food and fluid intakes in rats in each group were observed every other day and the data were displayed in Table 1. Before diabetes model formation, high-fat fed DM and DM+METF rats had higher fluid and food intakes (Table 1) as well as body weight gain (Fig. 1A) compared to that in control rats. After diabetes model

Table 1 Fluid and food intake in rats in each group

Groups	Fluid intake (mL/d)	Food intake (g/d)	Weight gain (g/day)
Con Group			
Before STZ injection	23.00 ± 3.00	19.40 ± 0.20	2.63 ± 0.10
After STZ injection	24.00 ± 4.00	20.20 ± 0.70	2.58 ± 0.30
DM Group			
Before STZ injection	40.00 ± 5.00 [a]	26.70 ± 0.40 [a]	3.95 ± 0.40 [a]
After STZ injection	115.00 ± 4.00 [a]	33.50 ± 0.50 [a]	1.81 ± 0.10 [a]
DM+METF Group			
Before STZ injection	39.00 ± 4.00 [a]	26.60 ± 0.50 [a]	3.70 ± 0.60 [a]
After STZ injection	32.00 ± 3.00 [ab]	24.30 ± 0.30 [ab]	-1.28 ± 0.30 [ab]

Data are means ± SEM for twenty animals in each group. Comparisons among three groups were achieved *via* one-way analysis of variance (ANOVA) followed by Dunnett's test [a] $p<0.05$ *versus* Con rats. [b] $p<0.05$ *versus* DM rats. Con Group: control rats group; DM Group: HFD/STZ induced diabetic rats group; DM+METF rats: HFD/STZ induced diabetic rats supplemented with metformin treatment.

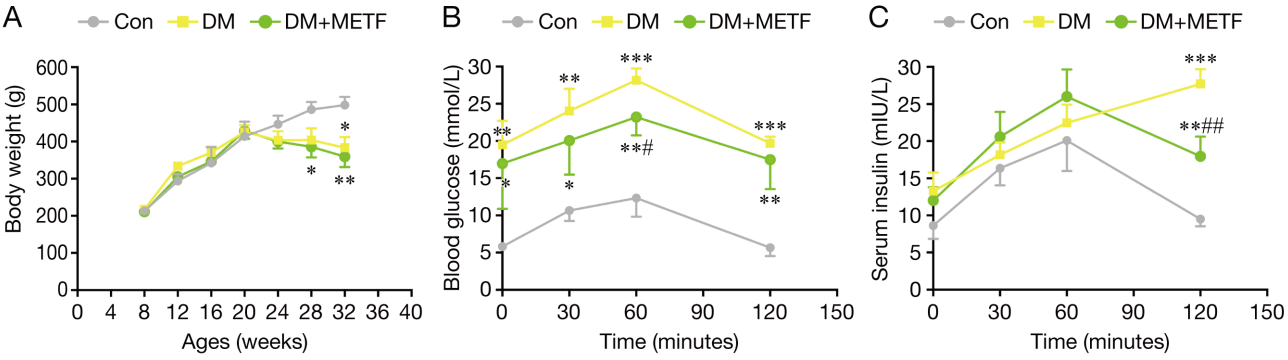

Fig. 1 Effects of metformin on high-fat fed/streptozotocin (HFD/STZ) induced diabetic rats

Diabetes was induced in Wistar rats and then administered with or without metformin (500 mg·kg^{-1}·d^{-1} p.o. for 12 weeks, n=20 per group). Body weight in control rats group (Con), HFD/STZ induced diabetic rats group (DM) and metformin treated DM rats group (DM+METF) were recorded every other day and showed every four weeks (**A**). At the age of 32 weeks, rats were fasted for 16 hours. Oral glucose tolerance test was performed and blood glucose (**B**) and serum insulin (**C**) at different time points were recorded. Data are means ± SEM. Comparisons among three groups were achieved *via* one-way analysis of variance (ANOVA) followed by Dunnett's test. * indicates that the mean is significantly different compared with that of Con rats. # indicates that the mean is significantly different compared with that of DM rats (* $p < 0.05$; ** $p < 0.01$; *** $p < 0.001$; # $p < 0.05$; ## $p < 0.01$).

formation, DM and DM+METF rats showed lower body weights than that in Con rats despite excessive fluid and food intakes. The typical symptoms of ploy phagia, polydipsia, and polyuria were observed in diabetic rats. After metformin treatment, DM+METF rats showed relatively decreased body weight compared to that in DM rats. The mechanisms by which metformin exerts body-lowering effects are still in a discussion. Some suggested that metformin can induce hypothalamic leptin receptor expression and increase central leptin sensitivity which then inhibits food intake [17]. Others suggested that changed gastrointestinal physiology and circadian rhythm by metformin could also affect food intake, fat oxidation and storage [18].

Effects of metformin on glucose, insulin and lipid profiles

The rational for choosing HFD/STZ rats as T2DM model was based on previous studies [19, 20]. At the end of our experiment, oral glucose tolerance test (OGTT) was performed to detect glucose and insulin concentrations at different time points. It is apparent that at 0 minutes HFD with a low dose of STZ (30-35 mg/kg) injection induced DM rats had almost 3 fold higher of fasting blood glucose (FBG) (Fig. 1B) and almost 2 fold higher of fasting insulin (FIN) (Fig. 1C) than that in Con rats (All $p<0.05$). According to HOMA-IR index, DM rats showed significant insulin resistance (Table 2). After oral administration

Table 2 Biochemical parameters in rats in each group

Parameters	Con Group	DM Group	DM+METF Group
BW, g	498.15 ± 44.40	383.28 ± 63.68 [a]	359.40 ± 56.46 [ab]
FBG, mmol/L	5.83 ± 0.35	19.52 ± 2.95 [aa]	16.93 ± 6.34 [ab]
FIN, m IU/L	8.71 ± 0.86	13.07 ± 0.62 [a]	12.08 ± 0.22 [ab]
TG, mmol/L	1.43 ± 0.87	3.94 ± 1.15 [a]	4.47 ± 1.19 [a]
TC, mmol/L	2.14 ± 0.30	12.10 ± 3.69 [aa]	3.43 ± 1.74 [ab]
HDL, mmol/L	1.16 ± 0.23	2.11 ± 0.47 [a]	1.18 ± 0.29 [ab]
LDL, mmol/L	0.55 ± 0.11	7.34 ± 0.19 [a]	0.82 ± 0.43 [ab]
TBAs, umol/L	26.67 ± 0.93	101.75 ± 4.31 [a]	81.00 ± 3.46 [ab]
HOMA-IR index	2.21 ± 0.20	10.80 ± 0.43 [aa]	8.72 ± 1.12

Data are means ± SEM for twenty animals in each group. Comparisons among three groups were achieved *via* one-way analysis of variance (ANOVA) followed by Dunnett's test. [a] $p<0.05$, [aa] $p<0.01$ *versus* Con rats. [b] $p<0.05$ *versus* DM rats. Con Group: control rats group; DM Group: HFD/STZ induced diabetic rats group; DM+METF rats: HFD/STZ induced diabetic rats supplemented with metformin treatment. BW, body weight; FBG, fasting blood glucose; FIN, fasting insulin; TG, triglyceride; TC, total cholesterol; HDL, high density lipoprotein cholesterol; LDL, low density lipoprotein cholesterol; TBAs, total bile acids; HOMA-IR, homeostatic model assessment of insulin resistance.

of glucose (2 g/kg), DM rats had higher glucose concentrations at each time point (Fig. 1B) and delayed insulin peak (Fig. 1C) than that in Con rats resembling the pathophysiological state of T2DM. After metformin treatment for 12 weeks, FBG in DM+METF rats (16.93 ± 6.34 mmol/L) was significantly reduced compared to DM rats (19.52 ± 2.95 mmol/L), but still higher than Con rats (5.83 ± 0.35 mmol/L) (Table 2, Fig. 1B). Besides, DM+METF rats showed reduced FIN and improved glucose-induced insulin response, indicating that insulin sensitivity was improved after metformin treatment (Table 2, Fig. 1C).

Lipid profiles were also impaired in DM rats with total triglyceride (TG) and low density lipoprotein cholesterol (LDL-C) significantly increased (Table 2, All $p<0.05$). Metformin treatment significantly decreased serum levels of TG and LDL-C (Table 2, All $p<0.05$). Moreover, total bile acids (TBAs) and total cholesterol (TC) were significantly decreased after metformin treatment (Table 2, All $p<0.05$), suggesting that the cholesterol efflux was improved.

Metformin exerts opposite effects on FGF19 and FGF21 in diabetic rats

At 32 weeks of age, FGF19 serum level was reduced (Fig. 2A, $p<0.05$), while FGF21 was increased in DM rats (Fig. 2B, $p<0.05$), indicating that FGF19 and FGF21 metabolisms were in disorders in T2DM. However, after metformin treatment, we detected a continuous decrease of FGF19 and an increase of FGF21 in DM+METF rats compared to DM rats (Fig. 2A, 2B, All $p<0.05$). The opposite alterations of FGF19 and FGF21 in DM+METF rats may suggest that metformin regulates FGF19 and FGF21 in different manners.

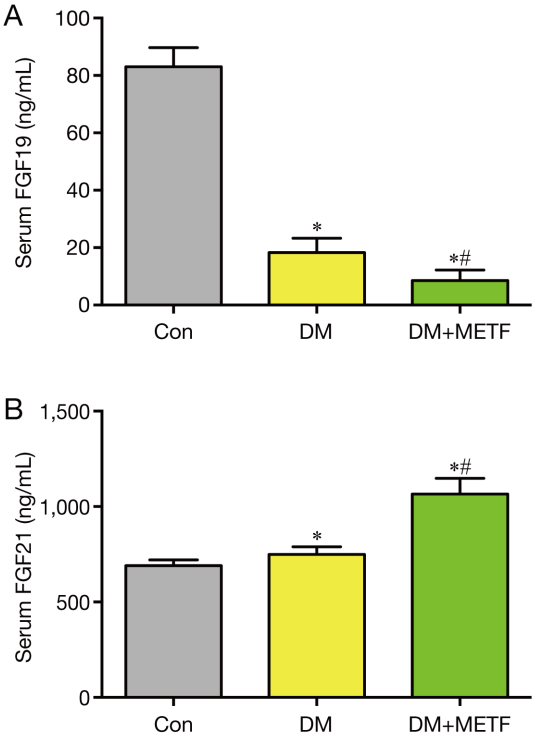

Fig. 2 Opposite regulations of FGF19 and FGF21 by metformin

Diabetes was induced in Wistar rats and then administered with or without metformin (500 $mg \cdot kg^{-1} \cdot d^{-1}$ p.o. for 12 weeks, n=20 per group). At the age of 32 weeks, rats were fasted for 16 hours. Serum FGF19 (**A**) and FGF21 (**B**) in each group were analyzed by ELISA kits. Data are expressed as means ± SEM (n=4). Comparisons among three groups were achieved *via* one-way analysis of variance (ANOVA) followed by Dunnett's test. * indicates that the mean is significantly different compared with that of Con rats (* $p<0.05$). # indicates that the mean is significantly different compared with that of DM rats (# $p<0.05$).

FGFR1 in the pancreas and visceral adipose tissues in each group

Given the opposite alterations of FGF19 and FGF21 serum levels in DM+METF rats, we detected their metabolic receptor FGFR1. Since FGFR1 is mainly expressed in the pancreas and visceral adipose tissues, we subjected both tissues from each group to Western blot (WB) analysis. To our surprise, FGFR1 was significantly increased both in the pancreas (Fig. 3A) and visceral adipose tissues (Fig. 3B) in DM rats compared to control rats (All $p<0.05$). In DM+METF rats, FGFR1 was almost remained at a normal level in the pancreas (Fig. 3A), while still significantly increased in visceral adipose tissues compared to DM rats (Fig. 3B, $p<0.05$), suggesting that metformin's action on FGFR1 expression is tissue-specific. Since FGFR1 is predominantly expressed in β cells, we took the approach of IHC in the pancreas showing that FGFR1 immunostaining with brown granular deposits was observed in the cytoplasm and nuclei of Con rats (Fig. 4A). Strong FGFR1 immunostaining was observed in DM rats (Fig. 4B). Immunohistochemical results were quantified by IOD values using the Image-Pro Plus software (Fig. 4D). After metformin treatment, FGFR1 immunostaining was almost remained at a normal level (Fig. 4C), which was in accordance with WB results.

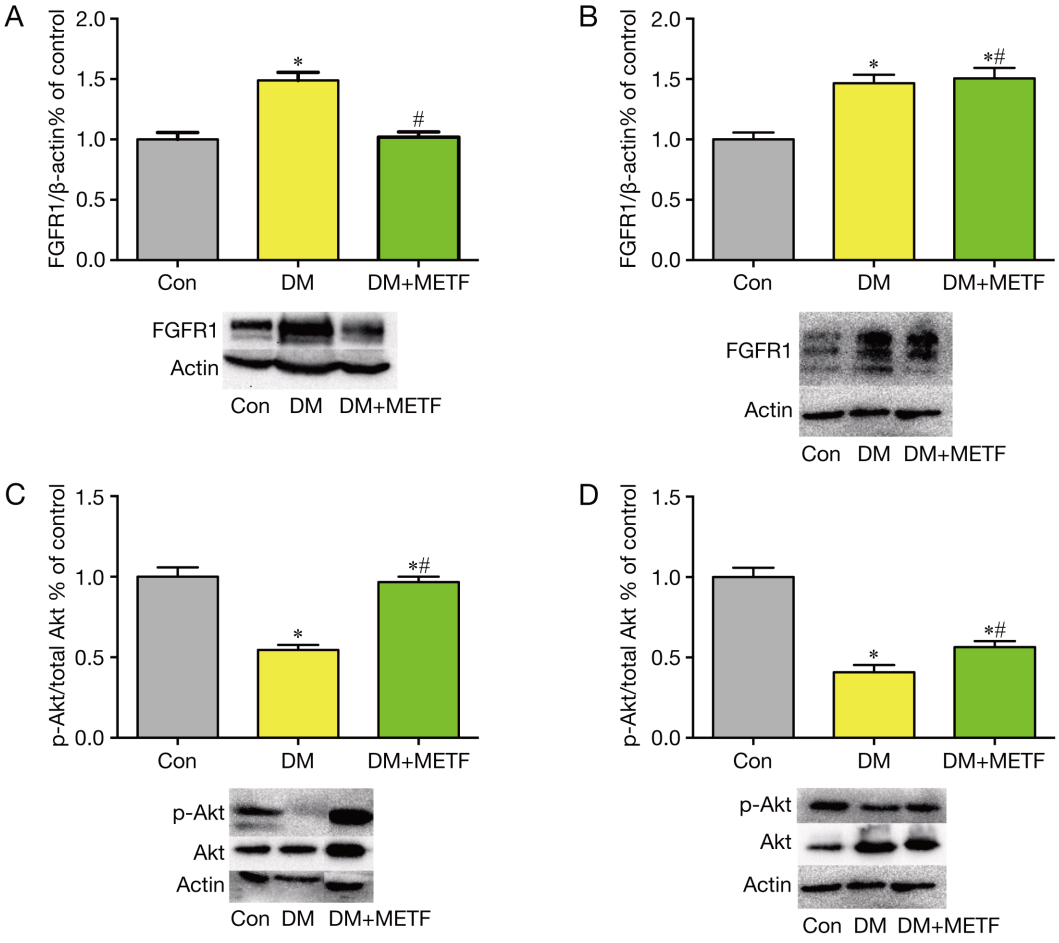

Fig. 3 Effects of metformin on FGFR1 expression and Akt phosphorylation in the pancreas and visceral adipose tissues

Diabetes was induced in Wistar rats and then administered with or without metformin (500 $mg \cdot kg^{-1} \cdot d^{-1}$ p.o. for 12 weeks, n=20 per group). Protein levels were determined by Western blot (WB) and were quantified with Image J. Quantification of FGFR1 in the pancreas (**A**) and visceral adipose tissues (**B**); phospho-Akt in the pancreas (**C**) and visceral adipose tissues (**D**). Data shown are representative of 3-5 independent experiments. Comparisons among three groups were achieved *via* one-way analysis of variance (ANOVA) followed by Dunnett's test. * indicates that the mean is significantly different compared with that of Con rats ($p < 0.05$). # indicates that the mean is significantly different compared with that of DM rats ($p < 0.05$).

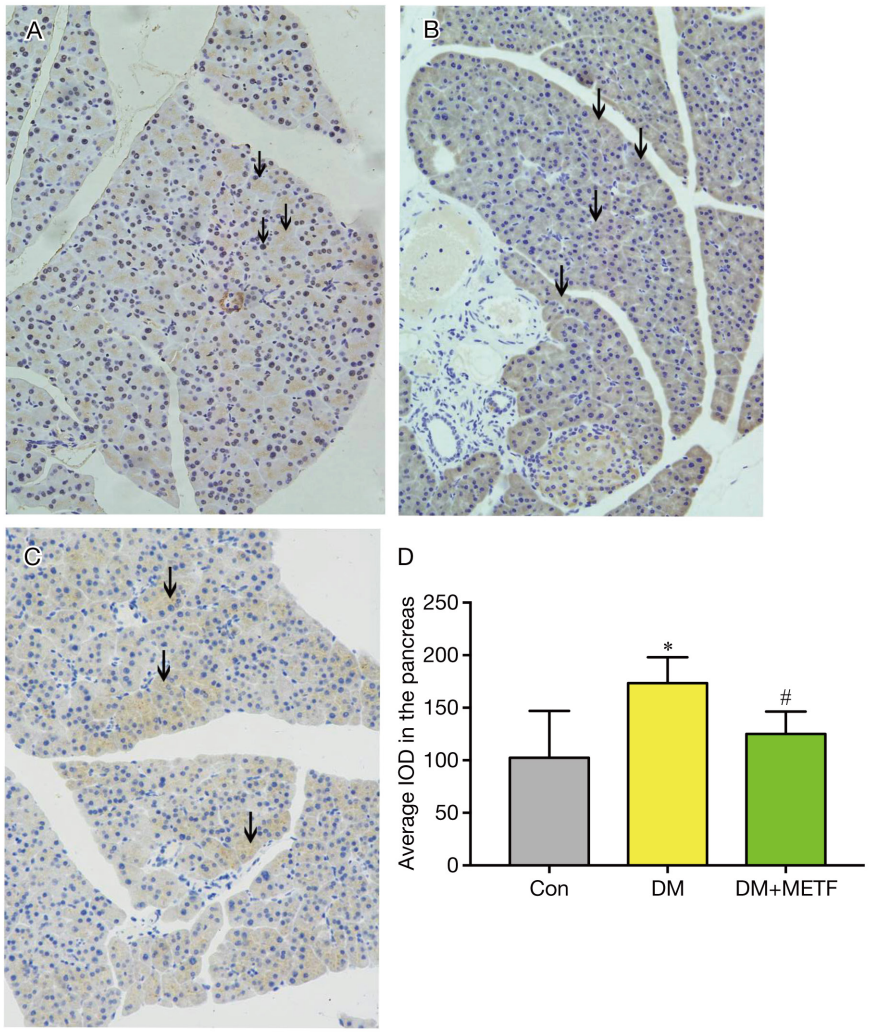

Fig. 4 Representative immunohistochemical staining and quantitative analysis of FGFR1 in the pancreas were shown at a magnification of 200×

(**A**) Immunostaining for FGFR1 with brown granular deposits in the cytoplasm and nuclei of Con rats. (**B**) Strong FGFR1 immunostaining in DM rats. (**C**) FGFR1 immunostaining with brown granular deposits was almost reached to a normal level in the cytoplasm and nuclei of DM+METF rats. (**D**) Protein levels of FGFR1 were determined by immunohistochemistry (IHC) and were quantified with Image-Pro Plus software by comparing IOD values. Data are expressed as means ± SEM. Comparisons among three groups were achieved *via* one-way analysis of variance (ANOVA). * indicates that the mean is significantly different compared with that of Con rats ($p < 0.05$). # indicates that the mean is significantly different compared with that of DM rats ($p < 0.05$).

Akt phosphorylation in the pancreas and visceral adipose tissues in each group

Akt is an important kinase during metabolic and gen regulatory response. Besides, PI3K/Akt is also a major celluar transduction signaling pathway involved in insulin sensitivity and β-cell functions. Moreover, recent study suggested that the FGFs-FGFRs binding also activates Akt pathways thus mediating metabolic effects. Herein, we detected Akt phosphorylation to find out possible mechanism underlying metformin treatment. We subjected pancreatic (Fig. 3C) and visceral adipose tissues (Fig. 3D) to Akt and phospho-Akt anti-bodies to detect the phosphorylation of Akt in each group. The phosphorylation of Akt was decreased in both tissues in DM rats compared to Con rats (All $p<0.05$). However, in DM+METF rats, Akt phosphorylation was elevated in both tissues compared to DM rats (Fig. 3C, 3D, All $p<0.05$).

Discussion

Metformin acts on metabolic signaling pathway *via* AMPK mechanisms. Recent finding suggested that metformin could also interact with mammalian target of rapamycin complex 1 (mTORC1) signaling as well as pancreatic and duodenal homeobox 1 (PDX1) thus affecting pancreatic functions [21]. Besides, metformin has been shown to affect Farnesoid X Receptor (FXR) activities through AMPK-FXR crosstalk [22]. However, several studies on the effects of metformin on FXR activity are controversial. On one hand, metformin has been shown to phosphorylate FXR and inhibit its target genes [22]. On the other hand, several studies suggested that metformin could induce FXR target gene such as FGF21 expression in an AMPK-dependent pathway [23, 24]. In the present study, we took the approach to generate the *in vivo* study in HFD/STZ induced type 2 diabetic rats, and investigated the effect of metformin on FXR target genes such as FGF19 and FGF21 and combined their metabolic receptor FGFR1 to find out possible mechanisms.

Insulin resistance and decreased insulin secretion have been shown to be characteristics of T2DM. In our study, T2DM rat model was induced by feeding rats with HFD and a low dose of STZ (30-35 mg/kg). Generally, the β cell toxin STZ has been used in both type 1 and type 2 diabetes animal model. However, the dose of STZ is important in diabetes model formation. Several researches have demonstrated that HFD-fed rats with a low dose of STZ (30-35 mg/kg) is considered to represent the pathophysiological state of T2DM, while a high dose of STZ (45-55 mg/kg) resembled more like type 1 diabetes [20]. At the end of the experiment, HFD/STZ diabetic rats displayed increased blood glucose at each time point and delayed serum insulin peak. As such, HFD/STZ treated rats are in a state of insulin resistance and still capable of secreting substantial amount of insulin.

At 32 weeks of age, metformin treatment (orally, 500 $mg \cdot kg^{-1} \cdot d^{-1}$) resulted in marked improvement of FBG as well as insulin resistance in HFD/STZ-diabetic rats, as has been previously demonstrated. Besides, lipid profiles such as LDL-C and TG were also improved after metformin treatment, although not to a standard level that was statistically significant. Moreover, bile flow was promoted with TC and TBAs reduced after metformin treatment (Table 2, All $p<0.05$). BAs are synthesized from cholesterol in the hepatocytes and regulated by the key enzyme *Cyp7a1*. In the physiological condition, the increased BAs activate its nuclear receptor FXR and then profoundly activate SHP transcription thus decreasing *Cyp7a1* and BA synthesis. In rat model of T2DM, TBAs were significantly increased and showed a metabolic disorder (Table 2). However, after metformin treatment, TBAs and TC were both significantly reduced, suggesting that the secretion and excretion of BAs are promoted. A possible explanation for these results is that metformin interacts with and inhibits FXR thus increasing *Cyp7a1* and bile acid transporters (*Besp* and *Mrp2*) [22]. Thus, our results suggest that administration of metformin in DM rat may increase bile flow favoring cholestasis.

Here, we confirmed that FGF19 was reduced and FGF21 was increased in HFD/STZ induced diabetic rats (Fig. 2, All $p<0.05$), which was similar to previous studies [7, 25]. Our current study shows that metformin administration exerts opposite effects on FGF19 (decrease) and FGF21 (increase) in DM+METF rats (Fig. 2). As regards FGF19, it has already been suggested that FGF19 is produced by the activation of FXR, the bile acid nuclear receptor; and Fleur Lien *et al*. suggested that FXR was mediated by metformin through AMPK-FXR crosstalk [22]. The mechanistic explanation for the reduced FGF19 in DM+METF rats may be that metformin inhibits FXR transcription thus inhibiting FGF19 production [22]. There are several mechanisms responsible for the increased FGF21 by metformin treatment. Some suggested that metformin induces FGF21 production in the liver in an activating transcription factor 4 (ATF4)-dependent way and inhibits mitochondrial respiration which is independent of AMPK and mTORC1 pathways [26]. Others suggested that metformin dose-dependently induces FGF21 expression in hepatocytes in an AMPK-dependent pathway [23]. A plausible explanation for the discrepancy may be that AMPK functions differently depending on its cell locations. Besides, a former study showed that FXR was important in mediating the increase of FGF21 [3]. While another study showed that metformin activated AMPK can phosphorylate and inhibit FXR as well as its target proteins [22]. We hypothesized that there may exist other mechanisms in mediating metformin and FGF21 actions which is independent of FXR.

For FGFR1, our present study using WB and IHC showed that FGFR1 was significantly increased both in the pancreatic β cells and visceral adipose tissues in

DM rats (Fig. 3A, 3B, Fig. 4, All $p < 0.05$), indicating the increased FGFR1 may be a compensatory response or a cause of T2DM. After metformin treatment, pancreatic FGFR1 expression was almost reached to a normal level. While in visceral adipose tissue, FGFR1 expression in DM+METF was increased compared to DM rats. However, the effects and mechanisms of metformin on FGFR1 have not been fully elucidated and further research is required. Previous study has shown that pancreatic and duodenol homeobox 1 (PDX1) is required for the expression of FGFR1 in the pancreas and metformin could induce PDX1 in embryonic pancreas [14]. Since PDX1 involves in the development and functions of β cells [14], the normalization of FGFR1 after metformin treatment may indicate the improved functions of β cells. Besides, gen analysis suggested that FGFR1 may be a regulator of adipogenesis by increasing fat cell numbers [27]. Moreover, our results confirmed the former hypothesis that the expression of FGFR1 was mediated by FGF21 circulating levels [28]. This research may provide an alternative to the problem of metformin therapy.

Since Akt signaling involves in β cell function and insulin sensitivity, the level of Akt phosphorylation may serve as a marker of the pancreatic function. In the present study, we observed a deteriorated signal transduction of Akt in the pancreas (Fig. 3C) and visceral adipose tissues in DM rats (Fig. 3D). After metformin treatment, Akt phosphorylation was restored in both tissues (Fig. 3C, 3D), and this may indicate improved insulin signaling in both tissues. Even though many factors can affect Akt signaling, we hypothesized that the restored Akt signaling is in some part resulted from the elevated FGF21 circulating level. Besides, Wente *et al*. showed that FGF21 improves β cell function and survival by activating Akt signaling pathway [29]. Further studies will be employed to discover the possible mechanism focusing on FGF21-FGFR1 binding effect.

In conclusion, the *in vivo* study demonstrates that administration of metformin to DM rats exerts additional effects such as increasing bile flow and elevating FGF21. Besides, for the first time we find that metformin affects FGFR1 both in the pancreas and visceral adipose tissues. Further exploring the FGFs-FGFRs binding effect of metformin will be useful for insight into novel therapeutic options.

Acknowledgements

This work was supported by Science and Technology Development Program of Shandong (Grants No. 2012GSF11803); Shandong Province Key R&D Plan (Grants No. 2016GSF201019).

Disclosure of Conflict of Interest

None.

References

1. Kim YD, Park KG, Lee YS, Park YY, Kim DK, *et al*. (2008) Metformin inhibits hepatic gluconeogenesis through AMP-activated protein kinase-dependent regulation of the orphan nuclear receptor SHP. *Diabetes* 57: 306-314.
2. Holt JA, Luo G, Billin AN, Bisi J, McNeill YY, *et al*. (2003) Definition of a novel growth factor-dependent signal cascade for the suppression of bile acid biosynthesis. *Genes Dev* 17: 1581-1591.
3. Cyphert HA, Ge X, Kohan AB, Salati LM, Zhang Y, *et al*. (2012) Activation of the Farnesoid X Receptor induces hepatic expression and secretion of fibroblast growth factor 21. *J Biol Chem* 287: 25123-25138.
4. Inagaki T, Choi M, Moschetta A, Peng L, Cummins CL, *et al*. (2005) Fibroblast growth factor 15 functions as an enterohepatic signal to regulate bile acid homeostasis. *Cell Metab* 2: 217-225.
5. Potthoff MJ, Boney-Montoya J, Choi M, He T, Sunny NE, *et al*. (2011) FGF15/19 regulates hepatic glucose metabolism by inhibiting the CREB-PGC-1-1α pathway. *Cell Metab* 13: 729-738.
6. Yu D, Ye X, Wu Q, Li S, Yang Y, *et al*. (2015) Insulin sensitizes FGF21 in glucose and lipid metabolisms via activating common AKT pathway. *Endocrine* 52: 527-540.
7. Jeon JY, Choi SE, Ha ES, Kim TH, Jung JG, *et al*. (2016) Association between insulin resistance and impairment of FGF21 signal transduction in skeletal muscles. *Endocrine* 53: 97-106.
8. Owen BM, Mangelsdorf DJ, Kliewer SA (2015) Tissue-specific actions of the metabolic hormones FGF15/19 and FGF21. *Trends Endocrinol Metab* 26: 22-29.
9. Perry RJ, Lee S, Ma L, Zhang D, Schlessinger J, *et al*. (2015) FGF1 and FGF19 reverse diabetes by suppression of the hypothalamic-pituitary-adrenal axis. *Nat Commun* 6: 6980.

10. Xu J, Lloyd DJ, Hale C, Stanislaus S, Chen M, *et al*. (2009) Fibroblast growth factor 21 reverses hepatic steatosis, increases energy expenditure, and improves insulin sensitivity in diet-induced obese mice. *Diabetes* 58: 250-259.
11. Wu X, Ge H, Lemon B, Weiszmann J, Gupte J, *et al*. (2009) Selective activation of FGFR4 by an FGF19 variant does not improve glucose metabolism in ob/ob mice. *Proc Natl Acad Sci U S A* 106: 14379-14384.
12. Foltz IN, Hu S, King C, Wu X, Yang C, *et al*. (2012) Treating diabetes and obesity with an FGF21-mimetic antibody activating the Klotho/FGFR1c receptor complex. *Sci Transl Med* 4: 162ra153.
13. Ge H, Baribault H, Vonderfecht S, Lemon B, Weiszmann J, *et al*. (2012) Characterization of a FGF19 variant with altered receptor specificity revealed a central role for FGFR1c in the regulation of glucose metabolism. *PloS One* 7: e33603.
14. Hart AW, Baeza N, Apelqvist A, Edlund H (2000) Attenuation of FGF signalling in mouse beta-cells leads to diabetes. *Nature* 408: 864-868.
15. Yang C, Wang C, Ye M, Jin C, He W, *et al*. (2012) Control of lipid metabolism by adipocyte FGFR1-mediated adipohepatic communication during hepatic stress. *Nutr Metab (Lond)* 9: 94.
16. Wu AL, Kolumam G, Stawicki S, Chen Y, Li J, *et al*. (2011) Amelioration of type 2 diabetes by antibody-mediated activation of fibroblast growth factor receptor 1. *Sci Transl Med* 3: 113ra126.
17. Lv WS, Wen Jp, Li L, Sun Rx, Wang J, *et al*. (2012) The effect of metformin on food intake and its potential role in hypothalamic regulation in obese diabetic rats. *Brain Res* 1444: 11-19.
18. Malin SK, Kashyap SR (2014) Effects of metformin on weight loss: potential mechanisms. *Curr Opin Endocrinol Diabetes Obes* 21: 323-329.
19. Skovso S (2014) Modeling type 2 diabetes in rats using high fat diet and streptozotocin. *J Diabetes Investig* 5: 349-358.
20. Srinivasan K, Viswanad B, Asrat L, Kaul Cl, Ramarao P (2005) Combination of high-fat diet-fed and low-dose streptozotocin-treated rat: a model for type 2 diabetes and pharmacological screening. *Pharmacol Res* 52: 313-320.
21. Gregg B, Elghazi L, Alejandro EU, Smith MR, Blandino-Rosano M, *et al*. (2014) Exposure of mouse embryonic pancreas to metformin enhances the number of pancreatic progenitors. *Diabetologia* 57: 2566-2575.
22. Lien F, Berthier A, Bouchaert E, Gheeraert C, Alexandre J, *et al*. (2014) Metformin interferes with bile acid homeostasis through AMPK-FXR crosstalk. *J Clin Invest* 124: 1037-1051.
23. Nygaard EB, Vienberg Sg, Orskov C, Hansen HS, Andersen B (2012) Metformin stimulates FGF21 expression in primary hepatocytes. *Exp Diabetes Res* 2012: 465282.
24. Kim EK, Lee SH, Jhun JY, Byun JK, Jeong JH, *et al*. (2016) Metformin prevents fatty liver and improves balance of white/brown adipose in an obesity mouse model by inducing FGF21. *Mediators Inflamm* 2016: 5813030.
25. Roesch SL, Styer AM, Wood GC, Kosak Z, Seiler J, *et al*. (2015) Perturbations of fibroblast growth factors 19 and 21 in type 2 diabetes. *PloS One* 10: e0116928.
26. Kim KH, Jeong YT, Kim SH, Jung HS, Park KS, *et al*. (2013) Metformin-induced inhibition of the mitochondrial respiratory chain increases FGF21 expression via ATF4 activation. *Biochem Biophys Res Commun* 440: 76-81.
27. Jiao H, Arner P, Dickson Sl, Vidal H, Mejhert N, *et al*. (2011) Genetic association and gene expression analysis identify FGFR1 as a new susceptibility gene for human obesity. *J Clin Endocrinol Metab* 96: E962-E966.
28. Suzuki M, Lee AY, Vazquez-Medina JP, Viscarra JA, Crocker DE, *et al*. (2015) Plasma FGF21 concentrations, adipose fibroblast growth factor receptor-1 and beta-klotho expression decrease with fasting in northern elephant seals. *Gen Comp Endocrinol* 216: 86-89.
29. Wente W, Efanov AM, Brenner M, Kharitonenkov A, Koster A, *et al*. (2006) Fibroblast growth factor-21 improves pancreatic beta-cell function and survival by activation of extracellular signal-regulated kinase 1/2 and Akt signaling pathways. *Diabetes* 55: 2470-2478.